❒   1530

Modeling load sensing pressure and flow control of axial piston pump by analyzing impact of bulk modulus

Vivek Verma[1], Sachin Kumar[2], Apurva Anand[3]
[1]Department of Mechanical Engineering, Amity School of Engineering and Technology, Amity University, Lucknow, India
[2]Department of Electronics Engineering, Amity School of Engineering and Technology, Amity University, Lucknow, India
[3]Maharana Pratap Engineering College, Kanpur, India

Article Info	ABSTRACT
	This research is focused on investigating the impact of the bulk modulus on the dynamics of variable delivery hydraulic axial piston pump (VAPP). The bulk modulus decreases exponentially with an increase in temperature whereas there is a linear positive relationship with pressure. The research revealed that there is a 6% (1 litre/s) increase in flow rate and a 2.6% (1.5 MPa) decrease in delivery pressure with a 38.75% (0.434 GPa) decrease in bulk modulus. Flow ripple and pressure pulsation are reduced by 39.3% and 43.2% respectively with a corresponding 38.75% decrease in bulk modulus. Pressure pulsation and flow ripple are responsible for the generation of noise and vibrations in the system. Flow rate increase contributes to better response and control of the VAPP. While a reduction in bulk modulus offers improved dynamic performance and overall response of the VAPP, it is noteworthy that a decrease in bulk modulus hurts the pump delivery pressure. The research allows the pump designer to formulate a strategy to optimize the bulk modulus under dynamic operating conditions to achieve optimal pump performance.

Corresponding Author:

Vivek Verma
Department of Mechanical Engineering, Amity School of Engineering and Technology, Amity University
Lucknow, India
Email: vverma@lko.amity.edu

1. INTRODUCTION

Axial piston pump (APP) acoustic emissions are often considered a major stumbling block intrinsic to fluid power systems. A principal genesis of the noise relates to flow ripples stemming from the functioning of positive displacement pumps. The periodic variation in flow rate and delivery pressure induces vibrations within the hydraulic system, generating oscillations in the variable delivery hydraulic axial piston pump (VAPP). These oscillations are primarily attributable to the pulsatile force within the pump, leading to vibrational patterns in the pump housing. Notably, the vibration can result in undesirable consequences such as elevated noise levels, potential fluid leakage, and structural fatigue. Hydraulic systems are vital in the industry, but their flow ripple and pressure fluctuations can affect the dynamics of the VAPP. Researchers have made progress in reducing these issues. The objectives of this study are derived from the extensive literature survey given as follows:
− To investigate bulk modulus variation with temperature and pressure in VAPP.
− Impact of bulk modulus on flow characteristics of VAPP.
− Impact of bulk modulus on flow ripple and pressure pulsation affecting VAPP dynamics and vibration.

– Suggest ways to enhance VAPP performance by reducing noise and vibration-inducing fluid flow phenomena.

Mathematical representation of the dynamic behavior of VAPP by simulating flow ripple and pressure pulsation characteristics enables the design of noise-optimized configurations [1]. Pettersson *et al.* [2] demonstrated the precompression filter volume method proving the most effective method to mitigate flow ripples. The Manring recommends reducing the nominal fluid volume within piston chambers by employing filled or capped pistons to reduce flow fluctuations due to piston backfilling during the transition from the intake port to the discharge port [3]. A novel timing mechanism was developed to diminish delivery flow ripple in APP under fixed-speed conditions across a wide range of operating conditions [4]. A critical aspect of noise and ripple reduction is determining the actual value of the source flow ripple. Researchers have developed an experimental 2 pressure/2 system method verified with theoretical predictions, enhancing accuracy [5].

The innovative tools CASPAR and AVAS developed to design port plate that effectively reduce swash plate oscillations while maintaining low flow ripple [6]. Kim *et al.* [7] successfully reduced pump noise by optimizing the pre-compression angle and introducing a notch design in the valve plate. With the new computer-based method, the valve plate design can be optimized before making a prototype [8]. An innovative multi-parameter, multi-objective optimization method (MOOM) was introduced for creating port plates to address fluid and structure-borne noises (FBN and SBN) in VAPP [9], [10]. An inventive design formulated for the transition region of the valve plate, in attenuating flow fluctuations while eliminating pressure fluctuations, for low-noise open-circuit VAPP [11]. Researchers effectively used a genetic algorithm-based MOOM to find the optimized port plate parameters that reduce both FBN and SBN levels [12]. Optimizing the parameter of pressure relief grooves by MOOM results in smaller flow ripples, making them more effective than ordinary precompression and decompression angles [13]. A study on the pre-pressurization fluid path, which includes a damping hole, a buffer chamber, and an orifice, aimed to optimize the design of a VAPP [14]. Hong *et al.* [15] developed a structure-optimizing method for a triangular damping groove on the outlet port of the port plate. This method considered multiple parameters of discharge flow rate to effectively reduce flow ripples.

The parametric optimization, involving the pre-pressure rising angle, cross angle, V-groove wrap angle, vertex angle, and opening angle, resulted in a remarkable 70.8% reduction in the maximum pressure gradient and a 21.4% decrease in flow fluctuations, showcasing its effectiveness [16]. Researchers have explored effective strategies for noise reduction, including well-designed relief grooves and the use of reactive silencers such as accumulators, in-line silencers, and side-branch resonators. There is also an alternative perspective suggesting that pump noise primarily results from shaft torque ripple, highlighting the need to minimize shaft torque fluctuations instead of focusing solely on flow ripples [17]. Researchers have developed a theoretical model to assess the impact of adjusting the volume of silencing grooves as a valuable design strategy for reducing pressure and flow fluctuations [18]. The application of open-loop control methods through electric drives has demonstrated potential for reducing flow ripples in hydraulic systems [19]. To gain a deeper understanding of the impact of cavitation on flow pulsation, researchers effectively employed computational fluid dynamics [20].

The dynamic analysis of swash plate vibration and pressure pulsation based on fluid-structure interaction (FSI) models has shown that the full FSI model is more accurate in predicting the swash plate vibration and pressure pulsations than non-FSI models. Discharge pressure pulsation is predominantly dictated by the kinematic relations of the piston slipper-shoe units (FSI-1), and isolated from swash plate vibration [21]. Investigation into the effect of swash plate active vibration control on pump noise emission confirmed that simultaneous sound pressure level reduction is achievable with minimal swash plate acceleration reductions [22]. To minimize the ripple in the outlet flow from the piston pump, the structural parameters in the pre-compression region are optimized as design variables. After optimization, the ripple in the outlet flow rate is significantly reduced at different outlet pressures [23]. Research on flow pulsation characteristics found that increased load pressure can reduce the flow pulsation rate with a decrease in the response speed of the flow rate, affecting the stability of the hydraulic system. Increasing angular speed and/or the number of pistons in APPs can reduce the flow pulsation rate and enhance the response speed of the flow rate [24].

Passive control of pressure ripple in APPs through the introduction of a sinusoidal profile on the swash plate surface by developing a mathematical model that accurately describes piston kinematics, resulting in a significant reduction in pressure ripple [25]. An active pressure controller utilizing the filtered-x least mean square algorithm with delay compensation was designed to reduce pressure ripple, and proved to be effective for single and multi-frequency components, resulting in substantial reductions in amplitude [26].

The research and technological advancements in hydraulic system noise and flow ripple reduction offer a promising path toward quieter and more efficient hydraulic systems across various applications. These studies showcase a diverse range of strategies and innovations that address the complex challenges posed by

flow ripple and noise, contributing to the enhancement of hydraulic systems in the industrial landscape. By combining theoretical modeling, advanced control mechanisms, and innovative design approaches, researchers are working diligently to optimize the performance of hydraulic systems while minimizing their noise emissions and flow ripples.

The literature review reveals a notable gap in research, as no prior investigations have been conducted to examine the influence of the bulk modulus of fluid on flow characteristics, flow ripple, and pressure fluctuations of VAPP. Pressure variation is high at high discharge pressures, high rotation speeds, and greater inclination α of VAPP [27]. The instant flow rate Q_i is influenced predominantly by α (swash plate angular position) and pump rpm (N), for specified valve plate shape and geometry. Flow ripple and pressure fluctuation will also vary in sync with the α and N. However, to evaluate the impact of bulk modulus or compressibility on the flow characteristics, flow ripple, and pressure fluctuation an innovative approach is required by developing a correlation between bulk modulus and flow rate. The pressure and bulk modulus have a linear relationship that is well-known from fundamental principles of fluid mechanics.

2. MATHEMATICAL MODELLING

A computational model is created to evaluate the impact of bulk modulus on flow rate, delivery pressure, flow pulsation, and pressure ripple that affects dynamics of the VAPP with MATLAB/Simulink. There is a complex correlation that exists between the bulk modulus and discharge or flow pulsation, however, pressure and bulk modulus have positive linear relations established from fluid mechanics principles. With the increase in pressure, there is an increase in fluid bulk modulus. The increase in bulk modulus is attributed to an increase in volumetric strain. The bulk modulus decreases exponentially with an increase in temperature. The model employs these basic physical principles stated here.

Applying the fundamental principle of fluid mechanics, the volumetric rate of flow Q_d is computed as the multiple of angular velocity and dynamic volume displaced, as (1).

$$Q_d = V_d \times N = \frac{Nnr\pi D_p^2}{2} \tan \alpha \tag{1}$$

Where, V_d = dynamic volume displaced, N = rotational speed of cylinder block, n = piston count, r = circular pitch for pistons, Dp = piston dimension, α = angular displacement of piston.

The above formula computes the mean volumetric rate of flow. Whereas instantaneous volumetric flow rate Q (flow ripple) is the cumulative net flow from every piston connected to a delivery port, given as (2);

$$Q = \sum_{i=1}^{m} Q_i \tag{2}$$

where, m = no of pistons providing discharge at the instant.

Instant discharge Q_i is of the ith piston given as (3) [28];

$$Q_i = sign(P_i - P_d)C_d A_{insp} \sqrt[2]{\frac{2}{\rho}|P_i - P_d|} \tag{3}$$

where, P_i = pressure of the ith piston at the instant, P_d = delivery pump pressure, C_d = discharge coefficient, A_{insp} = instantaneous piston area for delivery as per valve plate and cylinder [28].
For piston 1 to 2 A_{insp} is computed as (4),

$$A_{insp} = R_g R \varphi_i \sin \theta_1 \arctan (R_g \varphi_i tg\theta_1 tg(\tfrac{\theta_2}{2})/R) \quad 0 < \varphi_i < 2\pi/9 \tag{4}$$

where, R_g = radial distance of pressure release recess, R = radius of discharge port, φ_i = i^{th} angular position of piston, $\theta_1 \, and \, \theta_2$ = angular depth and width of pressure release recess respectively.
For piston 2 to 3 A_{insp} is computed as (5),

$$A_{insp} = (r\varphi_i - 2R)\sqrt{rR\varphi_i - \frac{r^2\varphi_i^2}{4}} + 2R^2 \arcsin \left(\frac{r\varphi_i - 2R}{2R}\right) + \pi R^2 \quad 2\pi/9 < \varphi_i < 3\pi/9 \tag{5}$$

For piston 3 to 4 A_{insp} is computed as (6),

$$A_{insp} = \pi R^2 + 2R(\varphi_i - 2\delta)r \quad 3\pi/9 < \varphi_i < 4\pi/9 \tag{6}$$

For piston 4 to 5 A_{insp} is computed as (7),

$$A_{insp} = \pi R^2 + 2R\, \varphi_i r \quad 4\pi/9 < \varphi_i < 5\pi/9 \tag{7}$$

were, δ = transitional angular distance of discharge port.
From piston 5 to 6, A_{insp} is stationary.
From piston 6 to 7, A_{insp} computed by formula 6.
From piston 7 to 8, A_{insp} same as piston 2 to 3.
From piston 8 to 9, A_{insp} same as piston 1 to 2.
 The instant pressure inside the cylinder is given by Ivantysyn and Iavntysynova [28].

$$\frac{dP_i}{dt} = - \frac{K(\frac{\pi D_p^2}{4}\omega r \tan\alpha - Q_i - Q_l)}{(V_0 - r\frac{\pi D_p^2}{4}(1-\cos\varphi_i)\tan\alpha)} \tag{8}$$

The instant cylinder pressure w.r.t. to angular velocity ω of the cylinder block, with $\varphi = \omega t$ and $d\varphi = \omega dt$.

$$\frac{dP_i}{d\varphi} = - \frac{K(\frac{\pi D_p^2}{4}\omega r \tan\alpha - Q_i - Q_l)}{\omega(V_0 - r\frac{\pi D_p^2}{4}(1-\cos\varphi_i)\tan\alpha)} \tag{9}$$

Where, V_o = average volume of a cylinder at the instant tilt plate is vertical to axis of the cylinder, Q_l = leakage of the pump and K = compressibility = 1/bulk modulus.

$$Q_l = Q_{cp} + Q_{cv} + Q_{ssp} \tag{10}$$

 All leakage flows are assumed as viscous with a constant gap as proposed by Ivantysyn and Ivantysnova [28]. Leakage between Cylinder piston.

$$Q_{cp} = \frac{\pi D_p h_p^3}{12\mu(s_i + l_A)}(P_i - P_0) \tag{11}$$

Leakage between cylinder and valve plate.

$$Q_{cv} = \frac{h_v^3}{12\mu}\left[\frac{1}{\ln\left(R_2/R_1\right)} + \frac{1}{\ln\left(R_4/R_3\right)}\right](P_i - P_0) \tag{12}$$

Leakage between slipper and swash plate.

$$Q_{ssp} = \frac{\pi D_d^4 h_s^3}{\mu[6D_d^4 \ln\left(R_2/R_1\right) + 128 h_s^3 l_d]}(P_i - P_0) \tag{13}$$

Where, h_p = cylinder-piston clearance, h_v = valve plate and cylinder clearance, h_s = slipper/pitch-plate clearance, l_A = starting clearance, l_d = full piston span, μ = viscosity (dynamic), s_i = instant piston stroke, P_o = pressure in the case drain, v_i = instant velocity of the piston, R_1, R_2 = inside and outside radius of inner valve plate sealing gasket, R_3, R_4 = = inside and outside radius of outer valve plate sealing gasket, D_d = capillary hole dia across the piston, r_1, r_2 = inside slipper pad radius and outside slipper pad radius.
 The pressure pulsations are affected by reciprocating piston sinusoidal movement and compressibility of the fluid. Hence, pump discharge pressure, P_d, is given as (14),

$$Q - Q_{tv} = \frac{V}{K}\frac{dP_d}{dt} \tag{14}$$

where, V = volume between discharge port and flow control valve and Q_{tv} = flow control valve discharge.
 The "fluid bulk modulus" is the gradient of stress-strain curve also known as fluid's elasticity. The fluid compressibility (K) is reciprocal of the fluid bulk modulus. The "stress" associated with the fluid is defined as the ratio of instantaneous fluid pressure and the bulk strain defined by a change in fluid volume divided by the volume. In general, the gradient of stress-strain curve is described by (15):

$$dp_i = -\beta\frac{dV}{V} \tag{15}$$

β is the fluid bulk modulus and p_i is instantaneous pressure in the barrel given by (8) and (9). The mass associated with a volume of fluid as $m= \rho V$, ρ is the fluid mass-density, now differentiating m.

$$dm = d\rho V + \rho dV \tag{16}$$

The mass of fluid is invariable, (16) gives relation between fluid density and bulk modulus as (17).

$$\frac{dV}{V} = -\frac{d\rho}{\rho} \tag{17}$$

Substituting the result of (17) into (18), the bulk-modulus of fluid expressed as (18).

$$\beta = P_i \ln\left(\frac{\rho_0}{\rho}\right) \tag{18}$$

where ρ_0 is the mass density of the fluid when the pressure, P_i, is zero.
For hydrostatic transmission the effective bulk modulus has a complex relation with flow rate [29]:

$$\beta = \frac{P_i - P_d}{\ln\left(\frac{Q_{in} - Q_l}{Q_d}\right)} \tag{19}$$

Fluid isothermal bulk modulus is given in the (20) [30]:

$$\beta = \beta_0 \exp\left(-\alpha_l T\right) \tag{20}$$

β_0 is isothermal bulk modulus at 0 absolute temperature and α_l is coefficient of thermal expansion.

3. IMPLEMENTATION OF PROPOSED MODEL
3.1. Test rig description

Figure 1 represents a test rig specifically engineered for exploring the interplay between a VAPP and a standard controller, effectively carrying out load-detection and pressure-regulating operation. An intricate VAPP model considers piston interface to pitch plate and valve plate. The VAPP is driven by a rotational speed source. The "Pressure/Flow controller" subsystem, incorporates a fixed orifice for load sensing. Input signals guide the controller in adjusting pitch plate angle within the VAPP, regulating the pressure variations for flow modulator.
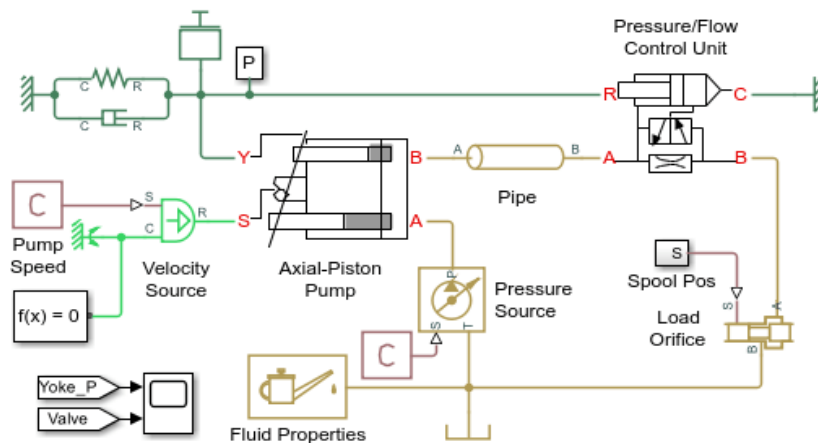
Figure 1. VAPP with load sensing pressure control [31]

3.2. Pump model

Piston pump model depicted in Figure 2 has nine piston assigned different ports proposed in the mathematical model for different phase angles. Suction openings are replicated through the utilization of the pressure source. The booster pump maintains an output pressure level set at 5 bars. The yoke is linked to the "Y" ports of all pistons, exerting its influence on the pitch plate mechanism.
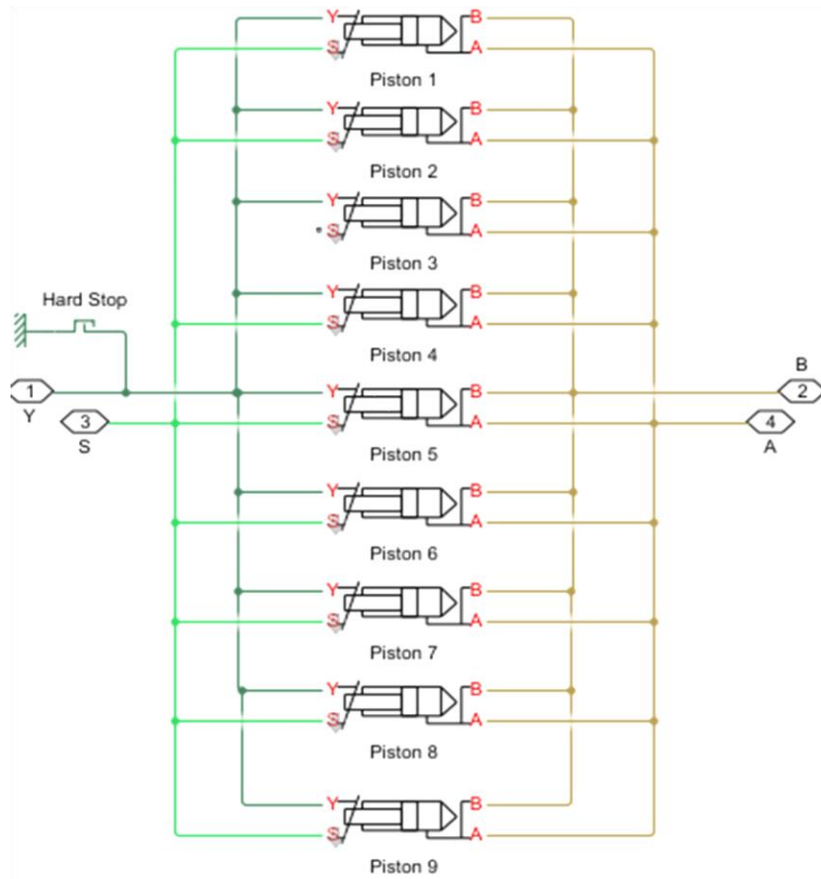
Figure 2. Piston assembly

3.3. Piston model

The piston's model, as depicted in Figure 3, relies on barrel motion. It is mechanically linked to the drive shaft via the pitch plate. Additionally, the barrel is interconnected with ports A and B using the "Porting plate variable orifice" blocks.
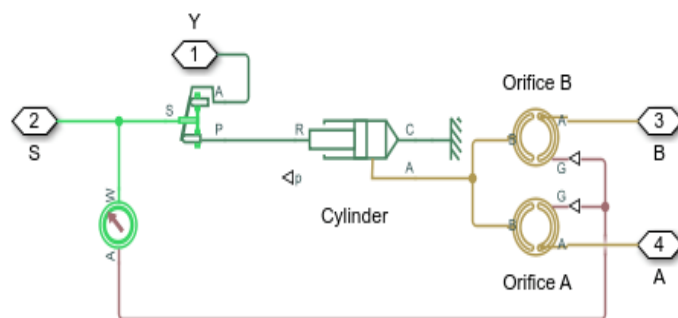
Figure 3. Piston model

4. RESULTS AND DISCUSSION

Theoretically analyzing in (18), it can be deduced that the bulk modulus increases with increasing pressure, attributed to the higher volumetric strain evident in the system, that causes higher pressure ripple in the VAPP. The relation between flow rate and bulk modulus is nonlinear in nature as evident from (19) and flow ripple increases with an increase in bulk modulus. Simulating the flow rate and instantaneous pressure

inside the chamber through MATLAB/Simulink utilizes data from Table 1, will substantiate the theoretical impact of bulk modulus on flow characteristics, flow ripple, and pressure pulsation.

Table 1. Simulation model parameters

Symbol	Value	Symbol	Value	Symbol	Value	Symbol	Value
n	9	R	4 mm	P_0	0 Pa	h_s	$15\mu m$
D_p	20 mm	C_d	0.72	h_v	$15\,\mu m$	d_d	2 mm
R	40 mm	V_0	17 cm^3	R_1	32.5 mm	r_1	6 mm
V	108 cm^3	h_p	$15\,\mu m$	R_2	35 mm	r_2	13 mm
V_s	0.45 m^3	μ	3.96×10^{-2} Pas	R_3	43 mm	l_d	67 mm
C_{dv}	0.65	l_A	15 mm	R_4	48 mm	ρ	962 kg/m^3
P_r	0 Pa						

4.1. Effect of temperature on bulk modulus
Figure 4 depicts a comparison between the Simulink data plot and the theoretical plot of bulk modulus variation with temperature as shown in Table 2. That is nonlinear as given in the (20) is consistent between the two. The fluid bulk modulus decreases exponentially with the increase in temperature that is also evident from in the (20).

Table 2. Bulk modulus variation with temperature

S. No.	Temperature (°C)	Bulk modulus (GPa)
1	60	1.12
2	70	1.06
3	80	1.00
4	90	0.953
5	100	0.903
6	110	0.854
7	120	0.809
8	130	0.766
9	140	0.725
10	150	0.686

4.2. Effect of pressure on bulk modulus
It can be visualized that the variation of bulk modulus with pressure is linear in nature shown in Figure 5. In (18) implies the linear relationship between bulk modulus and pressure. The increase in pressure corresponds to an increase in volumetric strain within the fluid, leading to the rise in bulk modulus.
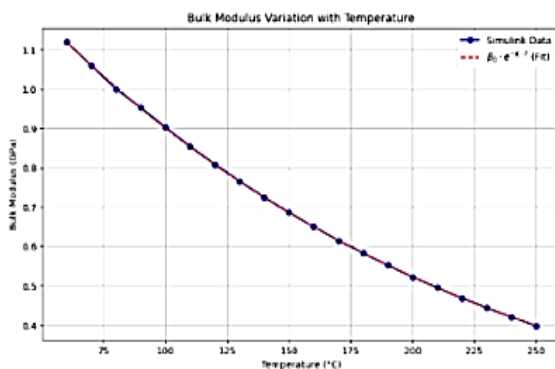
Figure 4. Bulk modulus variation with temperature
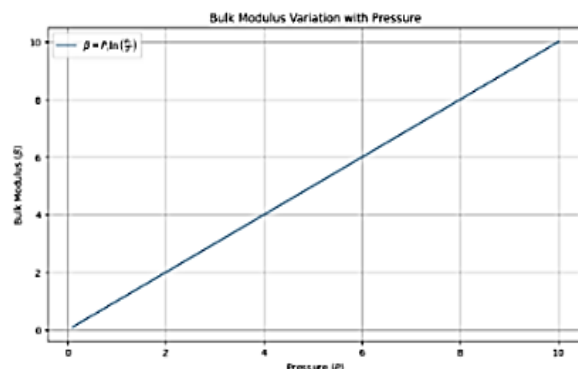
Figure 5. Bulk modulus variation with pressure

4.3. Effect of bulk modulus on discharge flow rate
The simulation model as presented in previous section with parameter depicted in Table 1, was employed for predicting the flow rates at varying bulk modulus settings illustrated in Figures 6 to 15. Figures 6 to 15 depict delivery flow rate fluctuation at varying bulk modulus of fluid which is temperature dependent by keeping rpm and α constant. Notably, it is evident that with the increase in temperature which decreases

fluid bulk modulus, there is an increase in the discharge flow rates. From the data analysis of the flow rate from Table 3 it can be observed that the mean flow rate increases by 6.5 percent with the decrease in the bulk modulus or increase in temperature from 60 °C to 150 °C. The quantified increase in flow rate is approximately 1 liter/s. pump output flow rate variation with bulk modulus (β).
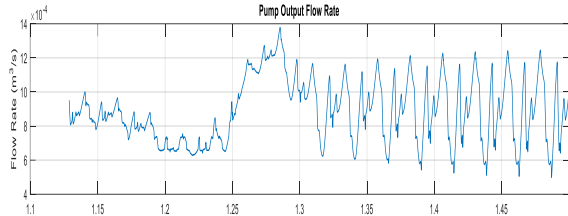
Figure 6. Discharge flow rate at β = 1.12 GPa
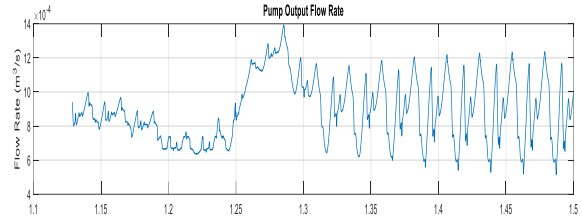
Figure 7. Discharge flow rate at β = 1.06 GPa
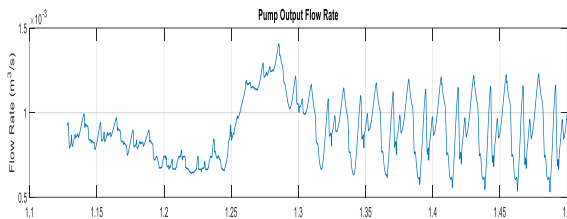
Figure 8. Discharge flow rate at β = 1.0 GPa
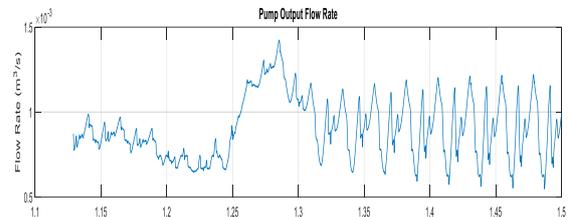
Figure 9. Discharge flow rate at β = 0.953 GPa
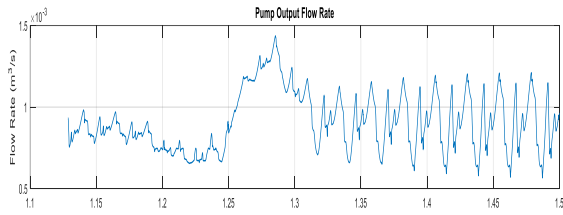
Figure 10. Discharge flow rate at β = 0.903 GPa
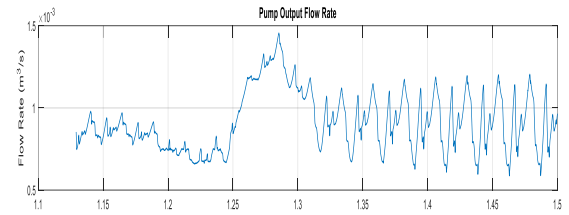
Figure 11. Discharge flow rate at β = 0.854 GPa
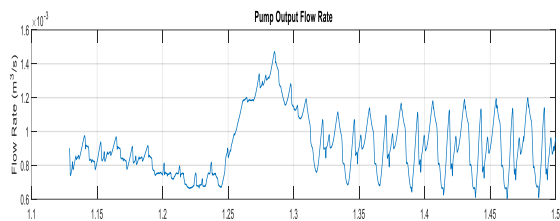
Figure 12. Discharge flow rate at β = 0.809 GPa
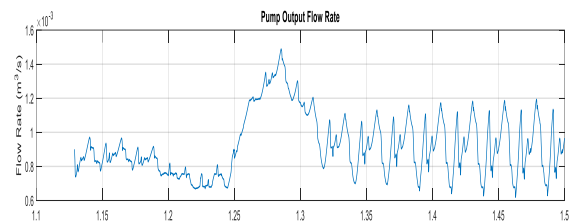
Figure 13. Discharge flow rate at β = 0.766 GPa
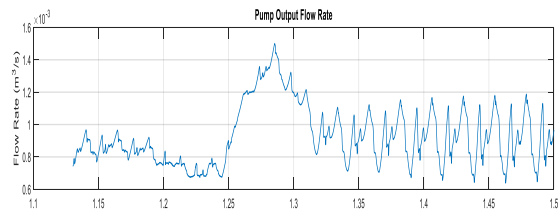
Figure 14. Discharge flow rate at β = 0.725 GPa
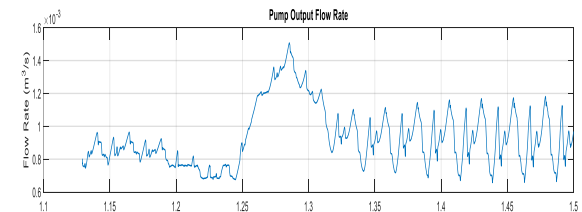
Figure 15. Discharge flow rate at β = 0.686 GPa

Table 3. The coefficient of flow ripples

β (GPa)	Q_{dmax}(m³/)	Q_{dmin} (m³/s)	C_{pf}	Avg (C_{pf})	β (GPa)	Q_{dmax}(m³/s)	Q_{dmin}(m³/s)	C_{pf}	Avg (C_{pf})
	0.00108	0.00062	0.541			0.00104	0.000710	0.377	
	0.00110	0.00063	0.543			0.00107	0.000733	0.373	
	0.00112	0.00061	0.596			0.00108	0.000673	0.464	
	0.00114	0.00058	0.651			0.00110	0.000664	0.494	
1.12	0.00115	0.00054	0.722	0.692	0.854	0.00112	0.000626	0.566	0.531
	0.00116	0.00052	0.762			0.00113	0.000608	0.600	
	0.00117	0.000511	0.784			0.00114	0.000595	0.628	
	0.00117	0.00050	0.802			0.00114	0.000586	0.642	
	0.00117	0.000498	0.827			0.00114	0.000589	0.637	
	0.00106	0.000652	0.477			0.00106	0.000775	0.328	
	0.00108	0.000645	0.504			0.00107	0.000760	0.339	
	0.0011	0.00062	0.558			0.00106	0.000687	0.425	
	0.0011	0.000598	0.591			0.00109	0.000684	0.458	
1.06	0.00114	0.000558	0.686	0.650	0.809	0.00111	0.000642	0.523	0.494
	0.00115	0.000541	0.720			0.00113	0.000624	0.577	
	0.00115	0.00052	0.754			0.00113	0.000612	0.595	
	0.00117	0.00052	0.769			0.00114	0.000615	0.598	
	0.00117	0.00051	0.781			0.00114	0.000612	0.603	
	0.00105	0.000642	0.482			0.00101	0.000710	0.348	
	0.00108	0.000665	0.476			0.00107	0.00087	0.305	
	0.0011	0.000635	0.536			0.00106	0.000699	0.404	
	0.00112	0.000616	0.581			0.00109	0.000695	0.443	
1	0.00114	0.000575	0.675	0.626	0.766	0.00110	0.000657	0.504	0.469
	0.00115	0.000558	0.693			0.00112	0.000640	0.545	
	0.00116	0.000545	0.721			0.00112	0.000638	0.548	
	0.00116	0.000536	0.736			0.00113	0.000632	0.565	
	0.00115	0.000532	0.735			0.00113	0.000633	0.564	
	0.00104	0.000648	0.464			0.00100	0.000740	0.299	
	0.00107	0.000686	0.437			0.00107	0.000816	0.269	
	0.00109	0.000647	0.510			0.00105	0.000713	0.382	
	0.00111	0.000633	0.547			0.00107	0.000706	0.410	
0.953	0.00113	0.000593	0.623	0.596	0.725	0.00110	0.000672	0.483	0.440
	0.00114	0.000576	0.657			0.00108	0.000655	0.490	
	0.00115	0.000563	0.685			0.00112	0.000642	0.543	
	0.00116	0.000535	0.737			0.00113	0.000640	0.554	
	0.00115	0.000553	0.701			0.00113	0.000653	0.535	
	0.00105	0.000660	0.456			0.00108	0.000790	0.310	
	0.00107	0.000708	0.407			0.00107	0.000840	0.241	
	0.00108	0.000660	0.483			0.00104	0.000726	0.356	
	0.00111	0.000649	0.524			0.00108	0.000718	0.403	
0.903	0.00113	0.000609	0.599	0.568	0.686	0.00109	0.000686	0.455	0.420
	0.00114	0.000592	0.633			0.00111	0.000696	0.458	
	0.00114	0.000578	0.654			0.00111	0.000656	0.514	
	0.00115	0.000569	0.676			0.00112	0.000658	0.520	
	0.00113	0.000664	0.520			0.00115	0.000666	0.530	

4.4. Effect of bulk modulus on delivery pressure

Figures 16 to 25 provide a representation of the delivery pressure at varying temperatures. The data analysis from Table 4 (see appendix) provides valuable insight into delivery pressure variation with bulk modulus. From the analysis, it can be deduced that delivery pressure is decreasing with a decrease in bulk modulus that is noteworthy till the temperature reaches 100 °C, without any change in α and rpm of the VAPP. After 100 °C there is no effect of temperature or bulk modulus on delivery pressure that remains constant and moves around 54.29 MPa till 150 °C. The decrease in delivery pressure is 6.5% with a 19.3% decrease in bulk modulus. Pump output pressure variation with bulk modulus (β).
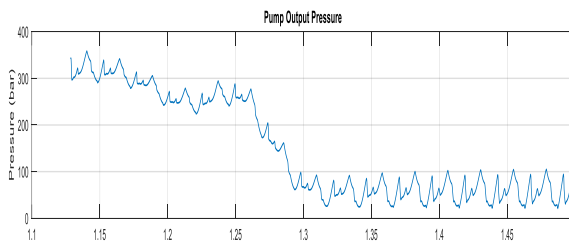
Figure 16. Pump discharge pressure at β = 1.12 GPa
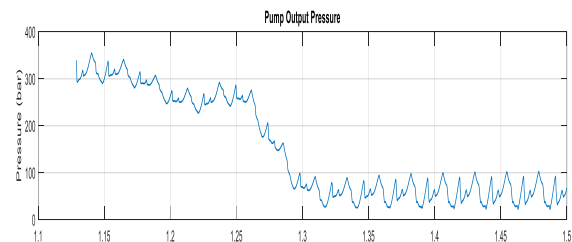
Figure 17. Pump discharge pressure at β = 1.06 GPa
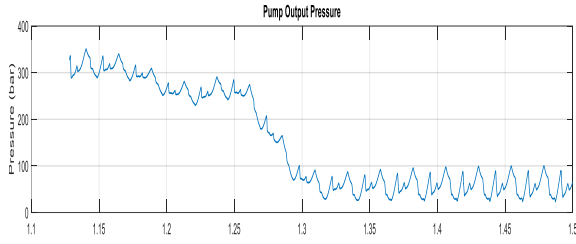
Figure 18. Pump discharge pressure at $\beta = 1.0$ GPa
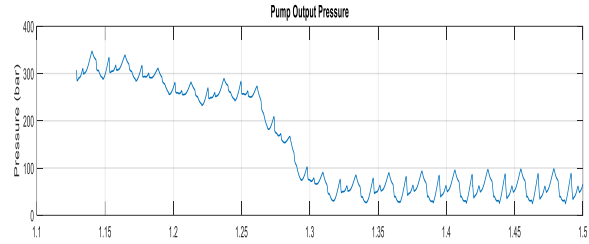
Figure 19. Pump discharge pressure at $\beta = 0.953$ GPa
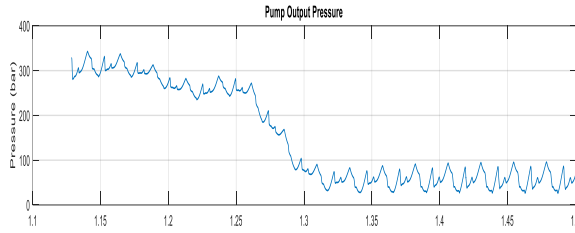
Figure 20. Pump discharge pressure at $\beta = 0.903$ GPa
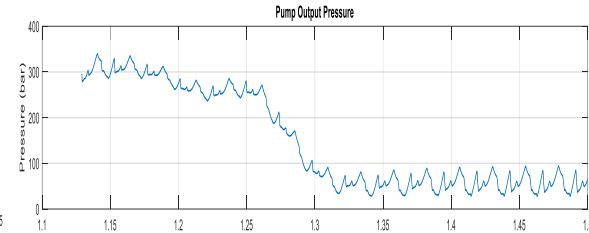
Figure 21. Pump discharge pressure at $\beta = 0.854$ GPa
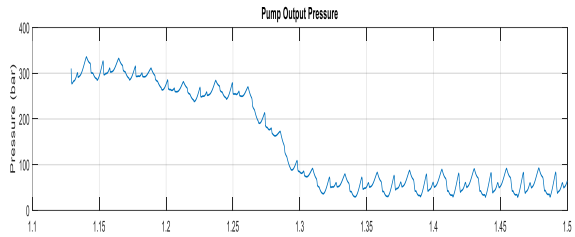
Figure 22. Pump discharge pressure at $\beta = 0.809$ GPa
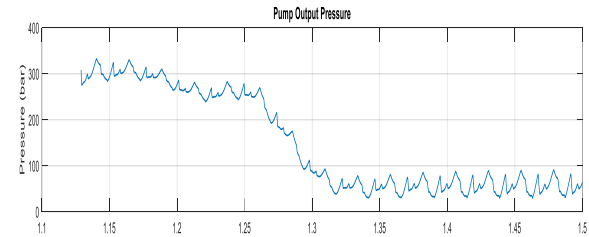
Figure 23. Pump discharge pressure at $\beta = 0.766$ GPa
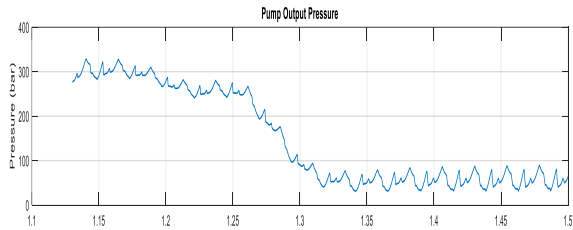
Figure 24. Pump discharge pressure at $\beta = 0.725$ GPa
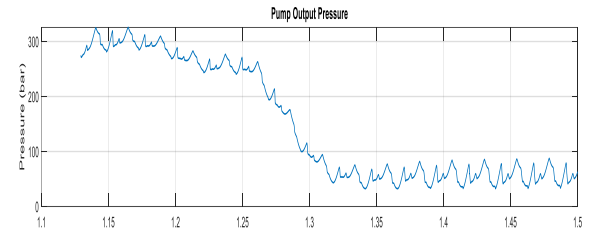
Figure 25. Pump discharge pressure at $\beta = 0.686$ GPa

4.5. Bulk modulus and flow ripple

To assess the impact of bulk modulus on flow ripples, a dimensionless parameter known as the coefficient of flow ripple (C_{fr}) is defined as (21):

$$\text{Coefficient of flow ripples, } C_{fr} = 2 * \frac{Q_{dmax} - Q_{dmin}}{Q_{dmax} + Q_{dmin}} \tag{21}$$

From the data analysis of Table 3, the flow ripple is decreasing with the decrease in bulk modulus or increase in temperature. Flow ripple reduction is notably significant at 39.30% with a corresponding 38.75% decrease in bulk modulus of fluid. The decrease in flow ripples with the decrease in bulk modulus can be attributed to less volumetric strain in the fluid. Figure 26 depicts the variation of flow ripple with bulk modulus β.

4.6. Bulk modulus and pressure pulsation

To evaluate the impact of bulk modulus on discharge pressure pulsations, a dimensionless parameter known as the coefficient of pressure fluctuation is defined as (22);

$$\text{Coefficient of pressure fluctuation, } C_{pf} = 2 * \frac{P_{dmax} - P_{dmin}}{P_{dmax} + P_{dmin}} \tag{22}$$

Pressure pulsation takes place because of the bulk modulus variation and the piston's reciprocating motion. Pulsation also depends on the number of the pistons. More the number of pistons more the pulsation. The pressure fluctuations originate within the transitional regions of the inner and outer dead center due to compression and expansion in the barrel. Data analysis from Table 4 and Table 2 can be deduced that pressure fluctuation is decreasing with the decrease in bulk modulus. The 38.75% decrease in bulk modulus proves to be reducing the pressure fluctuations by 43.2%. The decrease in pressure pulsation is attributed to a decrease in pressure that results in a less volumetric strain of the fluid depicted in Figure 27.
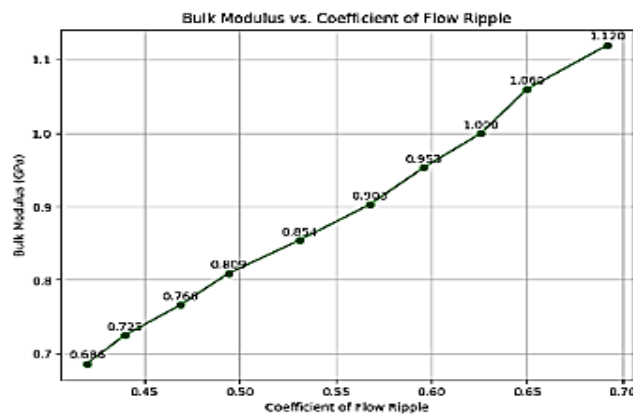
Figure 26. Flow ripple vs bulk modulus
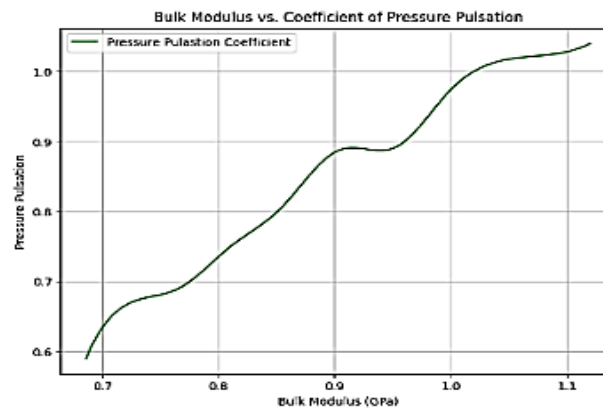
Figure 27. Pressure pulsation vs bulk modulus

5.   CONCLUSION

Simulating in the (20) that correlates bulk modulus with temperature, and plotting the data obtained of bulk modulus from the Simulink model are in agreement, demonstrating an exponential decrease in bulk modulus with an increase in temperature. Results obtained from simulating pressure and bulk modulus relation are coherent and align with established theory depicting positive linear correlation with no anomalies. There is a nonlinear relation between bulk modulus and flow rate. The simulation demonstrates a 6.5% increase in the flow rate of VAPP when the bulk modulus of the fluid decreased from 1.1 GPa to 0.59 GPa which quantifies to an increase of approximately 1 litre/s. The observed, increase in flow rate is significant for the better pump responsiveness given its critical nature of application in the aerospace

industry. A positive linear correlation between bulk modulus and pressure leads to a decrease in delivery pressure with the decrease in bulk modulus. The decrease in pressure is consistent till 100 °C temperature or 0.903 GPa bulk modulus and remains constant till 150 °C temperature or 0.686 GPa bulk modulus. The modest overall decrease in delivery pressure is 2.6% against a 39.2% decrease in bulk modulus. The dynamics of VAPP is influenced by flow ripple and pressure pulsation. It has been found that bulk modulus decreases, resulting in both flow ripple and pressure pulsation reduce significantly. Flow ripple and pressure pulsation reduce to 39.30% and 43.2% respectively corresponding to a 38.75% reduction in bulk modulus.

Optimizing the bulk modulus conditions within the operational range will be the key to enhancing pump efficacy. The fine balance between minimum delivery pressure drops and flow rate increase of the VAPP is key to achieving better performance of the pump. The acoustic noise and vibrations in the operation of VAPP that affect the dynamic performance of the pump is also improved because of the reduction in flow ripple and pressure pulsation. The reduction in bulk modulus has a major impact on the improved dynamic performance of the pump. These, findings of the research on the bulk modulus can help pump designers for designing control strategies that can dynamically adapt pump operation for optimal performance across a vast range of dynamic operating conditions. Also, research on the bulk modulus could pave the way for the development of new materials and fluids designed for use in VAPPs, further enhancing their dynamic performance.

APPENDIX

Table 4. The coefficient of pressure fluctuations

β(GPa)	P_{dmax}(N/m^2)	P_{dmin}(N/m^2)	C_{pf}	Avg(C_{pf})	β (GPa)	P_{dmax}(N/m)	P_{dmin} (N/m^2)	C_{pf}	Avg (C_{pf})
1.12	78.50	27.43	0.964	1.04	0.854	71.20	35.10	0.679	0.805
	80.50	26.34	1.014			72.29	34.01	0.694	
	84.94	24.54	1.103			73.97	29.15	0.869	
	88.00	23.48	1.158			77.90	29.01	0.915	
	90.4	22.68	1.198			80.71	28.67	0.951	
	92.10	21.93	1.230			82.60	28.43	0.976	
	93.14	21.40	1.253			83.55	27.87	1.000	
	93.87	21.81	1.246			84.30	27.25	1.023	
	93.17	21.56	1.248			84.79	27.74	1.014	
1.06	76.77	28.78	0.910	1.02	0.809	70.10	37.10	0.616	0.748
	78.97	27.42	0.969			71.36	36.18	0.654	
	82.77	25.48	1.058			72.08	29.70	0.833	
	84.71	24.65	1.098			76.25	30.00	0.871	
	88.37	24.30	1.137			79.06	29.78	0.906	
	90.05	23.12	1.183			79.98	29.24	0.929	
	91.00	22.69	1.202			82.11	29.04	0.955	91.00
	92.04	22.09	1.226			82.65	29.47	0.950	
1	75.50	29.95	0.864	0.974	0.766	69.70	39.60	0.550	0.690
	77.12	29.02	0.906			70.76	38.75	0.585	
	80.20	26.39	1.009			70.48	30.52	0.791	
	83.76	25.82	1.057			74.65	31.27	0.820	
	86.22	25.08	1.086			76.80	30.98	0.850	
	88.00	24.37	1.132			79.52	30.83	0.882	
	88.87	23.92	1.151			80.46	30.27	0.906	
	89.49	23.53	1.167			81.21	29.65	0.930	
	89.03	23.33	1.169			81.25	33.01	0.844	
.953	73.40	33.40	0.750	0.892	0.725	70.00	39.20	0.564	0.670
	75.48	30.41	0.851			71.42	40.96	0.542	
	77.95	27.35	0.961			68.90	31.53	0.744	
	81.18	26.93	1.004			72.31	31.94	0.774	
	84.30	26.30	1.049			76.03	31.90	0.818	
	86.17	25.88	1.076			77.10	31.48	0.840	
	86.95	25.20	1.101			79.07	31.54	0.859	
	87.65	24.77	1.118			79.54	31.48	0.866	
	86.98	24.56	1.119			79.56	31.87	0.802	
0.903	72.44	30.20	0.795	0.887	0.686	68.28	44.10	0.430	0.590
	73.81	32.23	0.784			71.21	43.29	0.488	
	74.75	27.95	0.911			67.43	32.32	0.704	
	78.60	28.01	0.949			71.03	32.38	0.748	
	82.43	27.50	0.999			73.92	32.85	0.769	
	83.10	27.15	1.015			76.61	32.54	0.810	
	85.27	26.34	1.056			77.79	32.19	0.829	
	85.58	25.98	1.068			78.78	32.66	0.828	
	86.38	26.35	1.065			79.05	32.15	0.844	

REFERENCES

[1]   D. N. Johnston and K. A. Edge, "Simulation of the pressure ripple characteristics of hydraulic circuits," *Proceedings of the Institution of Mechanical Engineers, Part C: Journal of Mechanical Engineering Science*, vol. 203, no. 4, pp. 275–282, Jul. 1989, doi: 10.1243/PIME_PROC_1989_203_114_02.

[2]   M. E. Pettersson, K. G. Weddfelt, and J. O. S. Palmberg, "Methods of reducing flow ripple from fluid power pumps - a theoretical approach," Sep. 1991, doi: 10.4271/911762.

[3]   N. D. Manring, "The discharge flow ripple of an axial-piston swash-plate type hydrostatic pump," *Journal of Dynamic Systems, Measurement and Control, Transactions of the ASME*, vol. 122, no. 2, pp. 263–268, Jun. 2000, doi: 10.1115/1.482452.

[4]   A. M. Harrison and K. A. Edge, "Reduction of axial piston pump pressure ripple," *Proceedings of the Institution of Mechanical Engineers. Part I: Journal of Systems and Control Engineering*, vol. 214, no. 1, pp. 53–63, Feb. 2000, doi: 10.1243/0959651001540519.

[5]   E. Kojima, J. Yu, and T. Ichiyanagi, "Experimental determining and theoretical predicting of source flow ripple generated by fluid power piston pumps," Sep. 2000, doi: 10.4271/2000-01-2617.

[6]   M. Ivantysynova, C. Huang, and S. K. Christiansen, "Computer aided valve plate design - an effective way to reduce noise," Oct. 2004, doi: 10.4271/2004-01-2621.

[7]   J. K. Kim, H. E. Kim, J. Y. Jung, S. H. Oh, and S. H. Jung, "Relation between pressure variations and noise in axial type oil piston pumps," *KSME International Journal*, vol. 18, no. 6, pp. 1019–1025, Jun. 2004, doi: 10.1007/BF02990874.

[8]   G. K. Seeniraj and M. Ivantysynova, "Impact of valve plate design on noise, volumetric efficiency and control effort in an axial piston pump," in *American Society of Mechanical Engineers, The Fluid Power and Systems Technology Division, FPST*, Jan. 2006, pp. 77–84, doi: 10.1115/IMECE2006-15001.

[9]   K. G. Seeniraj and M. Ivantysynova, "Multi-objective optimization tool for noise reduction in axial piston machines," *SAE International Journal of Commercial Vehicles*, vol. 1, no. 1, pp. 544–552, Oct. 2009, doi: 10.4271/2008-01-2723.

[10] G. K. Seeniraj and M. Ivantysynova, "A multi-parameter multi-objective approach to reduce pump noise generation," *International Journal of Fluid Power*, vol. 12, no. 1, pp. 7–17, Jan. 2011, doi: 10.1080/14399776.2011.10781018.

[11] B. Xu, Y. H. Sun, J. H. Zhang, T. Sun, and Z. B. Mao, "A new design method for the transition region of the valve plate for an axial piston pump," *Journal of Zhejiang University: Science A*, vol. 16, no. 3, pp. 229–240, Mar. 2015, doi: 10.1631/jzus.A1400266.

[12] S. G. Ye, J. H. Zhang, and B. Xu, "Noise reduction of an axial piston pump by valve plate optimization," *Chinese Journal of Mechanical Engineering (English Edition)*, vol. 31, no. 3, p. 57, Dec. 2018, doi: 10.1186/s10033-018-0258-x.

[13] B. Xu, S. Ye, J. Zhang, and C. Zhang, "Flow ripple reduction of an axial piston pump by a combination of cross-angle and pressure relief grooves: Analysis and optimization," *Journal of Mechanical Science and Technology*, vol. 30, no. 6, pp. 2531–2545, Jun. 2016, doi: 10.1007/s12206-016-0515-9.

[14] C. Guan, Z. Jiao, and S. He, "Theoretical study of flow ripple for an aviation axial-piston pump with damping holes in the valve plate," *Chinese Journal of Aeronautics*, vol. 27, no. 1, pp. 169–181, Feb. 2014, doi: 10.1016/j.cja.2013.07.044.

[15] H. Hong, C. Zhao, B. Zhang, D. Bai, and H. Yang, "Flow ripple reduction of axial-piston pump by structure optimizing of outlet triangular damping groove," *Processes*, vol. 8, no. 12, pp. 1–15, Dec. 2020, doi: 10.3390/pr8121664.

[16] S. Jian, L. Xin, and W. Shaoping, "Dynamic pressure gradient model of axial piston pump and parameters optimization," *Mathematical Problems in Engineering*, vol. 2014, pp. 1–10, 2014, doi: 10.1155/2014/352981.

[17] V. Mehta, "Torque ripple attenuation for an axial piston swash plate type," University of Missouri--Columbia, 2006.

[18] N. P. Mandal, R. Saha, and D. Sanyal, "Theoretical simulation of ripples for different leading-side groove volumes on manifolds in fixed-displacement axial-piston pump," *Proceedings of the Institution of Mechanical Engineers. Part I: Journal of Systems and Control Engineering*, vol. 222, no. 6, pp. 557–570, Sep. 2008, doi: 10.1243/09596518JSCE580.

[19] T. Minav, L. I. Laurilia, and J. Pyrhonen, "Axial piston pump flow ripple compensation by adjusting the pump speed with an electric drive," *The Twelfth Scandinavian International Conference on Fluid Power*, no. May 2011, 2011.

[20] H. Zhang, "Cavitation effect to the hydraulic piston pump flow pulsation," *Applied Mechanics and Materials*, vol. 599–601, pp. 230–236, Aug. 2014, doi: 10.4028/www.scientific.net/AMM.599-601.230.

[21] X. P. Ouyang, X. Fang, and H. Y. Yang, "An investigation into the swash plate vibration and pressure pulsation of piston pumps based on full fluid-structure interactions," *Journal of Zhejiang University: Science A*, vol. 17, no. 3, pp. 202–214, Mar. 2016, doi: 10.1631/jzus.A1500286.

[22] T. Kim and M. Ivantysynova, "Active vibration/noise control of axial piston machine using swash plate control," in *ASME/BATH 2017 Symposium on Fluid Power and Motion Control*, Oct. 2017, doi: 10.1115/FPMC2017-4304.

[23] X. Wu, C. Chen, C. Hong, and Y. He, "Flow ripple analysis and structural parametric design of a piston pump," *Journal of Mechanical Science and Technology*, vol. 31, no. 9, pp. 4245–4254, Sep. 2017, doi: 10.1007/s12206-017-0823-8.

[24] B. Wang and Y. Wang, "The research on flow pulsation characteristics of axial piston pump," in *Seventh International Conference on Electronics and Information Engineering*, Jan. 2017, vol. 10322, p. 103223O, doi: 10.1117/12.2265302.

[25] P. Casoli, M. Pastori, and F. Scolari, "Swash plate design for pressure ripple reduction - a theoretical analysis," in *AIP Conference Proceedings*, vol. 2191, p. 020038, 2019, doi: 10.1063/1.5138771.

[26] X. Huang, B. Xu, W. Huang, H. Xu, F. Lyu, and Q. Su, "Active pressure ripple reduction of a self-supplied variable displacement pump with notch least mean square filter," *Micromachines*, vol. 12, no. 8, p. 932, Aug. 2021, doi: 10.3390/mi12080932.

[27] J. M. Bergada, S. Kumar, D. L. Davies, and J. Watton, "A complete analysis of axial piston pump leakage and output flow ripples," *Applied Mathematical Modelling*, vol. 36, no. 4, pp. 1731–1751, Apr. 2012, doi: 10.1016/j.apm.2011.09.016.

[28] I. Jagadeesha and M. Ivantysynova, "Analysis of an axial-piston swash-plate type hydrostatic pump discharge flow characteristic," *Tech Books International*, 2003.

[29] N. D. Manring, "The effective fluid bulk-modulus within a ihydrostatic transmission," *Journal of Dynamic Systems, Measurement and Control, Transactions of the ASME*, vol. 119, no. 3, pp. 462–466, Sep. 1997, doi: 10.1115/1.2801279.

[30] S. Bair and P. Michael, "Modelling the pressure and temperature dependence of viscosity and volume for hydraulic fluids," *International Journal of Fluid Power*, vol. 11, no. 2, pp. 37–42, Jan. 2010, doi: 10.1080/14399776.2010.10781005.

[31] "The mathworks," *IEEE Signal Processing Magazine*, 2007. https://www.mathworks.com/help/hydro/ug/hydraulic-axial-piston-pump-with-load-sensing-and-pressure-limiting-control.html. (accessed Sep. 26, 2023).

BIOGRAPHIES OF AUTHORS

Vivek Verma 🆔 Ⓖ SC ◐ is a part-time research scholar at the Department of Mechanical Engineering at Amity School of Engineering and Technology, Amity University, Lucknow. He holds B.E. in Industrial Engineering and M.Tech in Production Engineering. Currently working as Assistant Professor at Department of Mechanical Engineering, Amity University, Lucknow, has 20 years' experience of teaching. He is member of several professional bodies such as SAE, IET (UK), and IAENG. He has research interest in Mathematical Modelling of Mechanical Systems and Computational fluid dynamics. He can be contacted at email: vverma@lko.amity.edu.

Sachin Kumar 🆔 Ⓖ SC ◐ is Ph.D in Electronics, M.Tech and B.E. in ECE, presently with Amity University, Lucknow. He has almost 20 years of academic and research experience. His research interest includes applications of Bio-Medical Signal Processing, AI/ML and Applications of Wireless Sensor Networks, He is an active member of number of professional bodies IEEE, IETE, IAENG, ISC, and IET(UK), he has published more than 80 research papers, book chapters, and articles in a number reputed Journal. He is an active member of editorial board/reviewer in various reputed journals. Dr Kumar has organized number of international conferences, has given invited talks, and chaired various technical sessions in conferences of repute. He can be contacted at email: skumar3@lko.amity.edu.

Apurva Anand 🆔 Ⓖ SC ◐ currently holds the position of Professor and Director at Maharana Pratap Engineering College, Kanpur, showcasing a career spanning over two dynamic decades. In his previous role, Dr. Anand served as the Professor and Dean at BBD University in Lucknow from 2017 to 2023. His academic journey includes key roles at ABES Engineering College and Amity Univeristy, where he served as Professor and Head of the Department. Holding a Ph.D. in Mechanical Engineering (ME) and Master's in ME and a Bachelor's in Industrial and Production Engineering. Dr. Anand's scholarly impact is evident in his 30 publications, garnering 401 citations with h-index of 05. Dr. Anand served as Program Chair for several conferences, actively guiding one Ph.D. scholar. He can be contacted at email: apurva2050@yahoo.co.in.